Proc. Natl. Acad. Sci. USA
Vol. 87, pp. 1203–1207, February 1990
Botany

Observation of a water-depletion region surrounding loblolly pine roots by magnetic resonance imaging

(*Pinus taeda*/mycorrhizae/rhizosphere)

J. S. MacFall*, G. A. Johnson†, and P. J. Kramer‡

*School of Forestry and Environmental Studies and ‡Department of Botany, Duke University, and †Department of Radiology, Duke University Medical Center, Durham, NC 27709

Contributed by P. J. Kramer, November 20, 1989

ABSTRACT **Magnetic resonance imaging was used to study sand containing various amounts of water and roots of loblolly pine planted into similar sand. Spin–lattice (*T1*) relaxation times of sand with water contents ranging from 0 to 25% (wt/wt) ranged from 472 to 1265 ms and increased with water content. Spin–spin (*T2*) relaxation times ranged from 54 to 76 ms and did not change in a discernible pattern with water content. Based on water content and measured *T1* and *T2* values, the signal intensity of sand/water images was predicted to increase with water content in a linear fashion, with the slope of the lines increasing with the time of acquisition repetition (*TR*). Measured signal intensity from images of sand with various water contents was found to follow a similar pattern. This allows interpretation of dark images of sand/water to be regions of low water content, and bright images to have comparatively greater water content. Images of loblolly pine seedling roots planted in identical sand showed the formation of a distinct water-depletion region first around the woody taproot and later showed the region extended and expanded around the lateral roots and clusters of mycorrhizal short roots. This observation strongly suggests that water uptake is occurring through the suberized region of the woody taproot.**

The relative amount of water and ions absorbed through various regions of roots has been a subject of discussion and investigation for several decades. The classical view was that water and probably ion uptake occurred chiefly in the unsuberized root hair zone just behind the tips of roots. However, the research of Kramer and Bullock (1) and Chung and Kramer (2) as well as several studies cited by them indicated that significant uptake of water and ions occurs through suberized regions of roots and woody plants. Haussling *et al.* (3) reported that water absorption occurs both near the tips and in older regions of Norway spruce roots, where lateral roots are emerging, and McCully and Canny (4) concluded that most of the water uptake by maize roots enters some distance behind the apical region.

Passioura (ref. 5 and references therein) expressed the concern that most measurements of water uptake were made on roots immersed in water rather than on roots growing in soil and usually were made on detached root segments or detopped root systems. The use of dyes to trace water movement into roots also creates problems due to selective uptake. Study of water and ion uptake by tree roots is complicated by the variety of roots that they possess, including taproots, various kinds of lateral roots, and mycorrhizal roots. This is illustrated by the differences in uptake observed by Haussling *et al.* (3).

Obviously, there would be significant advantages in observing water uptake by roots growing undisturbed in the soil and magnetic resonance imaging (MRI) makes this possible. Bottomley *et al.* (6) and Rogers and Bottomley (7) showed that it is possible to image roots in soil and other solid media, but they were unable to show quantitative changes in the water content of the root medium in which the roots were growing. Additional technical improvements have allowed detailed imaging of *in vivo* plant structure with some suggestive information of function (8–12).

Using these improved techniques, a series of experiments was conducted to observe the depletion of water from the immediate vicinity of roots on transpiring loblolly pine seedlings. This has demonstrated the ability to produce images that show water-depletion regions surrounding roots of various ages and sizes.

MATERIALS AND METHODS

To understand the effects of acquisition parameters on MRI images of water in sand, phantom studies were performed, using acid-washed quartz sand (sieved through a 60-mesh sieve) mixed with 0–25% (wt/wt) water. This sand was placed in 15-ml plastic centrifuge tubes, which were mounted in a Styrofoam holder and placed in a 6-cm-diameter horizontal coil. The tubes were imaged on a 2-tesla (T) General Electric Chemical Shift imager (CSI) model II imager, equipped with shielded gradients and housed at the Duke University Medical Center, Imaging Physics Laboratory. Images were reconstructed with a 256 × 256 array. Voxel size (the volume element comprising the image) was 0.36 × 0.36 × 2 mm. Five replicate phantoms were used to examine the relationship between spin density (water content of the sand) and signal intensity (image brightness). Spin–lattice relaxation time (*T1*) measurements were calculated from eight images of the same phantom with acquired repetition times ranging from 50 to 6000 ms. Spin–spin relaxation times (*T2*) were calculated from eight images with echo times ranging from 20 to 160 ms. Relaxation times were calculated from iterative fitting techniques (13). Four replicate sand phantoms were used for *T1* calculations and two were used for *T2* calculations.

Six-month-old container-grown loblolly pine seedlings (*Pinus taeda*) were donated by the North Carolina State Nursery at Clayton, NC. Seedlings were grown in the greenhouse for 2–4 months at Duke University, with a weekly fertilization of Peters Soluble Plant Food (20/20/20, N/P/K) (W.R. Grace, Fogelsville, PA). At the time of imaging, plants had a woody taproot, primary and secondary lateral roots, and both mycorrhizal and nonmycorrhizal short roots. The main mycorrhizal type was dark tan, with monopodial or dichotomously branching short roots, and had formed from natural inoculations. Prior to imaging, all but two lateral roots were excised from the tap root, and each seedling was transplanted

The publication costs of this article were defrayed in part by page charge payment. This article must therefore be hereby marked "*advertisement*" in accordance with 18 U.S.C. §1734 solely to indicate this fact.

Abbreviations: MRI, magnetic resonance imaging; *T1*, spin–lattice relaxation time; *T2*, spin–spin relaxation time; *TE*, echo time; *TR*, repetition time.

Downloaded at Palestinian Territory, occupied on November 28, 2021

into a 90 × 24 mm plastic container containing the same kind of sand used in the sand phantom. Seedlings were watered to saturation from the bottom of the container, and water was then allowed to drain freely. A piece of plastic tubing was attached with parafilm to the container bottom to allow watering of the seedling while inside the magnet. Tubes containing the seedling rooted in sand were placed into a 3-cm solenoid coil, which was placed vertically into the magnet bore. Conventional two-dimensional Fourier transform spin-echo imaging was used with echo time (*TE*) of 10 ms and repetition time (*TR*) of 600 ms. The total acquisition time for a single image was 10.2 min. Voxel size was 0.097 × 0.097 × 1.5 mm. Initial images were made within 2 hr of placement into the magnet bore. Sequential images were then made over a 24-hr period. During this time, the plants remained in the magnet without moving and were exposed to the overhead fluorescent lights. After 24 hr, plants were again watered to saturation of the sand from the bottom, water was drained, and plants were imaged again. Over a 2-month period, five replicate plants were prepared and imaged individually.

RESULTS AND DISCUSSION

Images of the sand phantom tubes showed that the brightness of the image increased with the water content (Fig. 1). *T1* values increased from 472 to 1265 ms with increasing water content (Fig. 2). *T2* values did not change in a discernible pattern and ranged from 54 to 76 ms (Fig. 2).

Other researchers have observed increasing *T1* values with increasing water content and a greater proportion of free water (which would increase *T1* values) (14). The measured values of *T1* are determined as the reciprocal of the summation of the proton components (primarily water in plant studies) of the material under study and can be determined by

$$1/T1 = (1/T1_1) + (1/T1_2) + (1/T1_3) + \ldots + (1/T1_n). \quad [1]$$

There may be many water components present; particularly in a heterogenous sample such as a root in soil, each with a separate value for *T1* ($T1_1 - T1_n$) and each exchanging protons. In fine sand, such as that used in this study, water is found in two states, tightly bound to the sand particles and free water within the interstitial spaces. There is no water inside the sand grains (5). Unless the water content of the sand is less than ≈5%, most of the water will be free water within the interstitial spaces and not tightly bound to the sand particles. This would, therefore, predict that as the water content of the sand increases, the measured *T1* values would also increase, as was found in the experiments reported here.

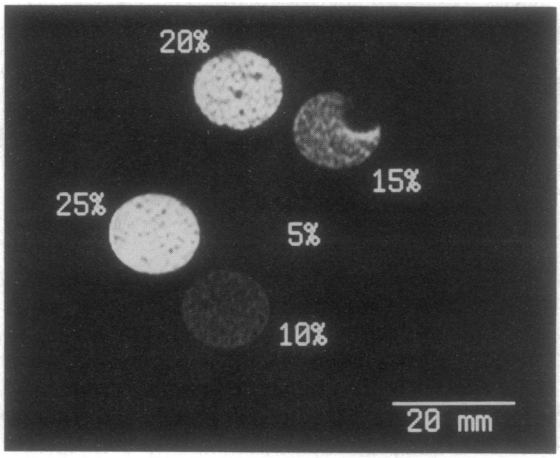

FIG. 1. MRI of sand phantom containing tubes of sand with the various water contents indicated.

For liquids, usually factors causing a reduction in *T1* values also cause a reduction in *T2* values. At this time it is not known why the *T2* values of the sand were found to be within a narrow range and did not change significantly with water content. A detailed study of the signal dependence of relaxation times (*T1* and *T2*) on water content is needed, but the phantom results assure a correct interpretation of signal dependence in the plant and sand images.

Interpretation of images obtained by MRI techniques is not necessarily dependent solely on water distribution patterns within the subject of study. The relationship between signal intensity and characteristics of proton distribution can be described by the function (15, 16)

$$S(^1\mathrm{H}) \propto N(^1\mathrm{H})(1 - e^{-TR/T1})e^{-TE/T2}, \quad [2]$$

where $S(^1\mathrm{H})$ is the signal intensity, $N(^1\mathrm{H})$ is the proton density, *TR* is the repetition time, and *TE* is the echo time.

Clearly there is not necessarily a linear relationship between image brightness and water content [$N(^1\mathrm{H})$]. Factors such as machine parameter settings during image acquisition (*TE* and *TR*) and inherent properties of the subject (*T1* and *T2*) determine image brightness. Additionally, as described for

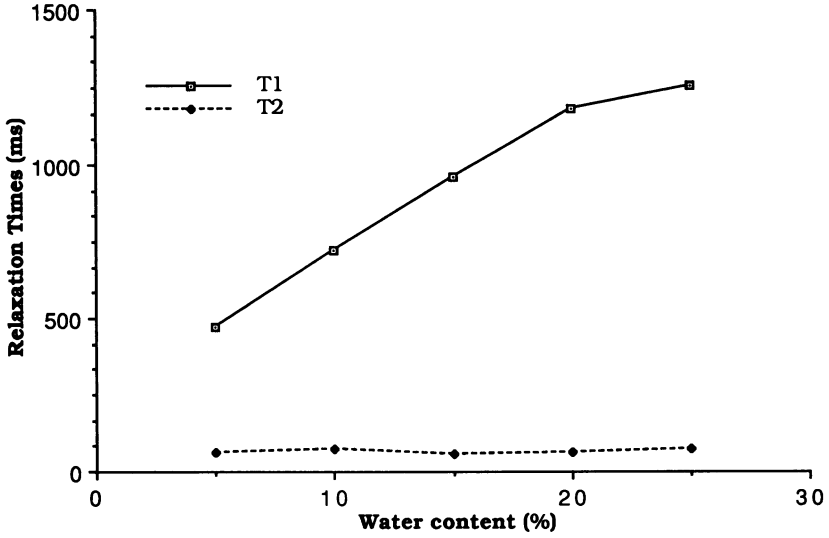

FIG. 2. *T1* and *T2* relaxation times of tubes of sand as affected by water content.

Downloaded at Palestinian Territory, occupied on November 28, 2021

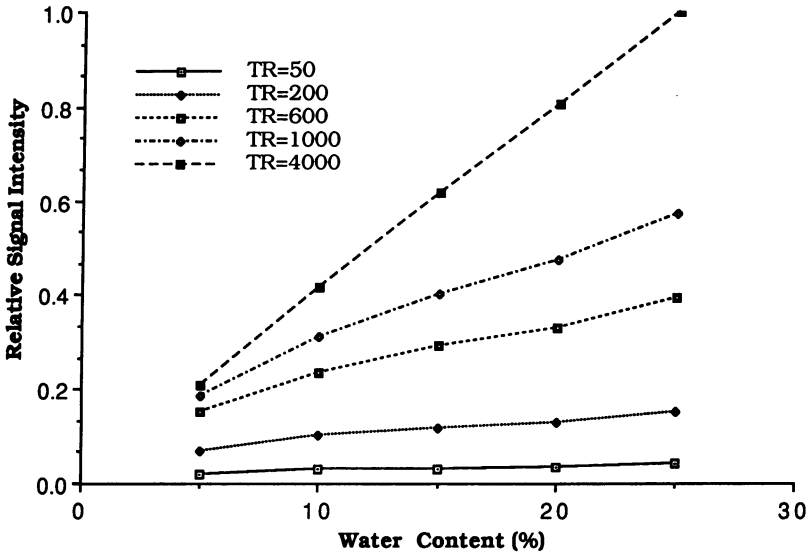

FIG. 3. Normalized predicted signal intensity of images of sand with various water contents calculated from measured *T1* and *T2* relaxation times and water content values.

sand of varied water contents, the value of *T1* changes with water content while *T2* values remain within a narrow range.

Substitution of measured water content and *T1* and *T2* values from the sand phantom experiment into Eq. 2 shows that for sand of various water contents the signal intensity increases linearly with water content (R^2 = 0.93–0.99) (Fig. 3). (Signal-intensity values have been normalized to a scale of 0–1 for both calculated and measured values.) The relationship is linear with the slopes increasing with *TR*. Measured signal intensity of sand phantom tubes of various water contents also increased with water content, as predicted, with greater slopes for greater values of *TR* (Fig. 4).

The sand phantom information allows interpretation of dark regions in sand images as regions of low water content and bright regions as areas of comparatively greater water content. Images of roots of transpiring seedlings planted into sand and imaged sequentially over time show dark areas around the taproots, which increase in diameter over time. These dark areas are regions of water depletion, as shown in Fig. 5. The depletion region is clearly visible first around the taproot with a small depletion region around the mycorrhizal short roots (Fig. 5*A*). The intensity profile across the image shows a sharp drop in signal intensity in the sand immediately adjacent to the taproot. In the subsequent image (Fig. 5*B*), the dark region has been extended and expanded to surround the mycorrhizal root cluster and the lateral root. This observation implies that the woody taproot, which has initiated secondary growth, is a region of water uptake by the seedling. A water-depletion region was observed to form around clusters of mycorrhizal short roots and around the lateral root, but clearly in this experiment the depletion region forms around the taproot soon after watering. It disappeared when the sand was rewatered (Fig. 5*C*).

Small pockets of dry sand or air were observed as dark areas within an otherwise relatively homogeneous sand image. This is seen as the dark round circle in the 15% water tube of the sand phantom (Fig. 1) and as three small dark circles in the upper portion of the sand imaged in Fig. 5 *A–C*.

Peak root growth of loblolly pines occurs in April and May, followed by a decline in growth throughout the summer and into winter (17). Transpiration of loblolly pines reaches a maximum during the warm summer months, during a period when the average rate of root elongation is declining (1, 17). In winter, while trees are still undergoing active transpiration, there is little new root growth to provide new unsuberized root tissue for water uptake (18). Even during the spring period of

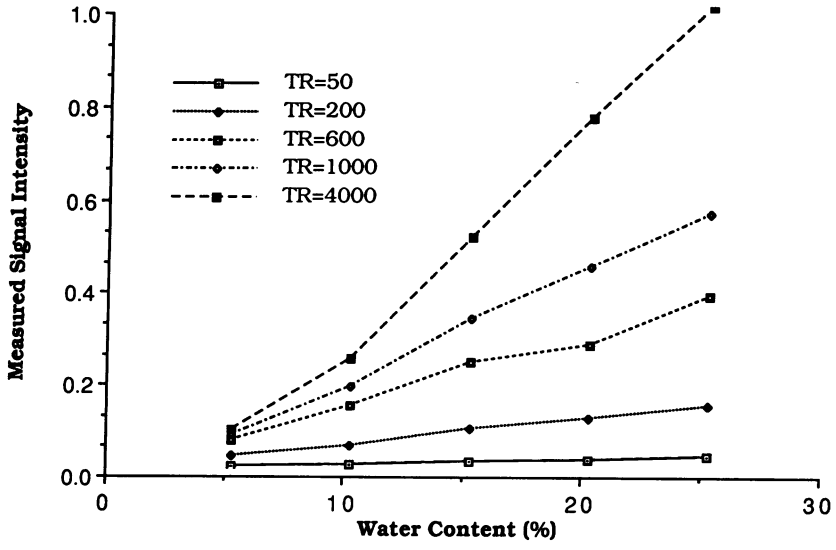

FIG. 4. Normalized mean measured signal intensity of sand with various water contents.

Downloaded at Palestinian Territory, occupied on November 28, 2021

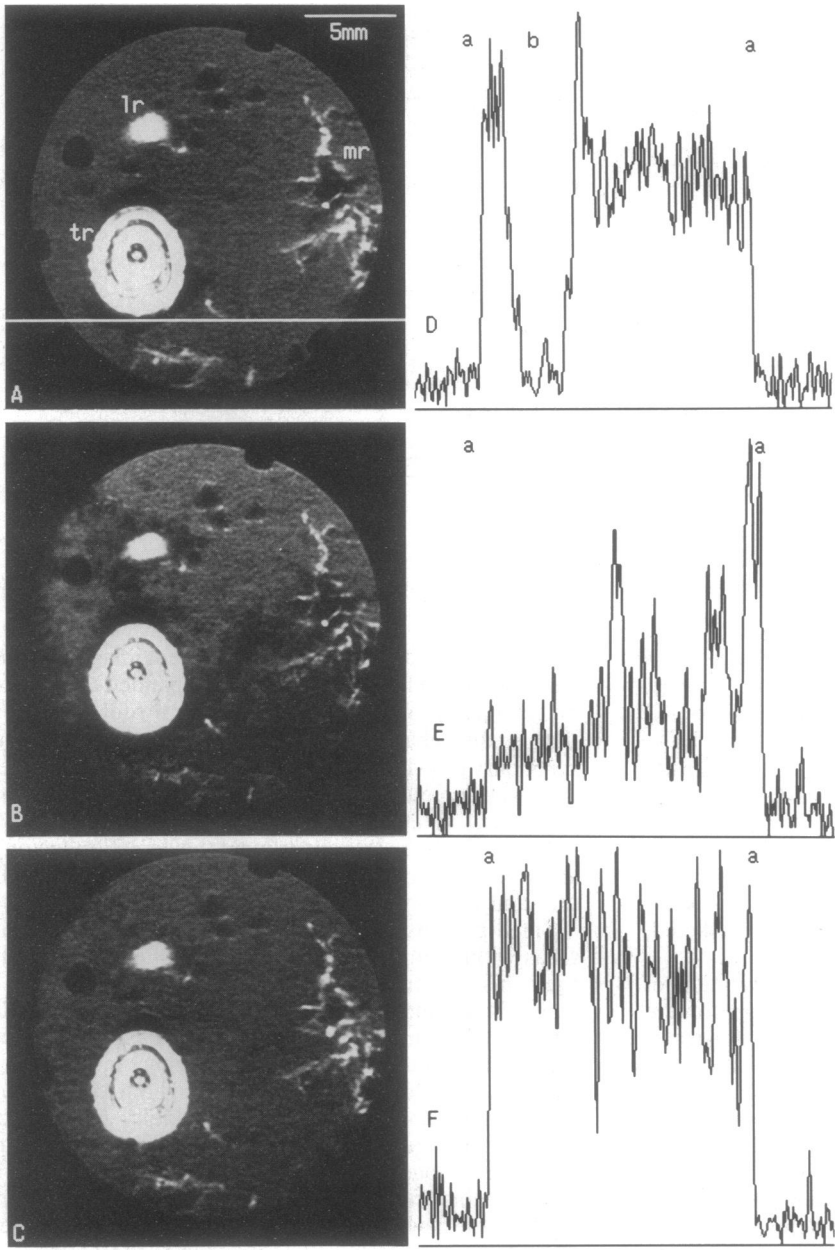

FIG. 5. Sequential MRI images of loblolly pine root about 15 mm below the soil surface. Slice thickness of projection is 1.5 mm; resolution is 0.097 mm. (*A*) At 2 hr after initial watering. (*B*) At 14 hr after initial watering. (*C*) Immediately after final watering. (*D*) Signal intensity profile at line shown in *A*, 2 hr after watering. (*E*) Signal intensity profile at 14 hr from watering. (*F*) Signal intensity profile immediately after final watering. tr, Taproot; lr, lateral root; mr, mycorrhizal roots; a, edge of container; b, edge of taproot.

most active elongation, root growth does not follow a pattern of continuous elongation but exhibits short periods of rapid growth followed by periods of depressed growth (17). The fluctuating pattern of elongation of roots would cause the unsuberized root surface area to be constantly changing even during periods of most active average root elongation. In contrast, the rate of transpiration by the tree increases through spring into summer in response to increasing soil temperatures and increasing canopy. This lack of coordination between patterns of root elongation and time of most active transpiration strongly suggests there are regions of water uptake by the tree other than unsuberized regions. As suggested by Chung and Kramer (2), it is likely that suberized woody regions are areas of water inflow. The images in the present work clearly show the formation of a water-depletion region surrounding the woody taproot, supporting the view that it as well as lateral roots and short roots participate in water uptake.

Other workers have observed uptake of dyes (3) into suberized roots through wounds or around emerging lateral roots. In the present study, junctures formed by vascular connections between the taproot and excised laterals were clearly visible in the MRI images. In Fig. 6, the depletion region was not only observed at the point of juncture between the two roots but extended around the perimeter of the taproot. Additionally, images were obtained of a containerized loblolly pine similarly transplanted into sand without excision of laterals (images not shown). A depletion region was observed to form first around the taproot and then extend down the lateral roots from the point of juncture, but was not restricted to the connective region around the taproot. The depletion region was later observed to extend to surround the numerous groups of mycorrhizal short roots and lateral roots remaining in the root plug. This suggests there are alternate paths for water inflow into woody root tissue other than through wounds or through the cambial disruption at the juncture region of branch roots to the axial roots.

No relationship was observed between the location of an excised lateral root and the formation of the water-depletion region. Although excised lateral roots seem likely to provide a path of reduced resistance to water flow at the root/soil interface, they do not appear to be the dominant path of water inflow into the taproot. As can be seen in Fig. 7, the depletion region surrounds the taproot and does not appear to have originated at the cut end of the excised root.

Downloaded at Palestinian Territory, occupied on November 28, 2021

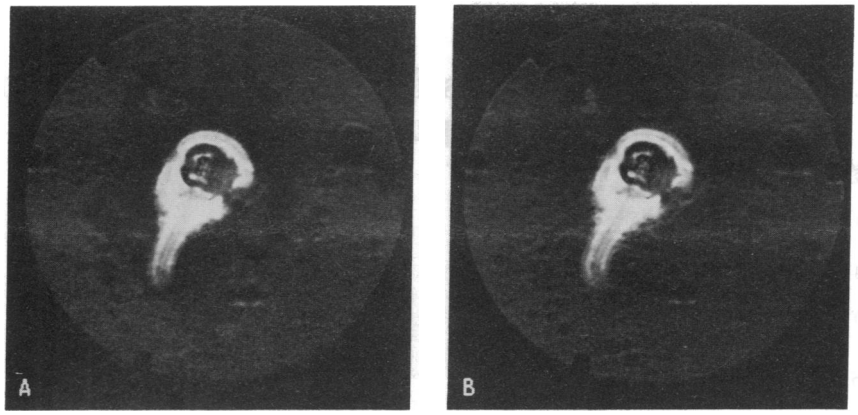

FIG. 6. Sequential images of loblolly pine taproot and intact lateral root. (*A*) At 24 hr after initial watering. (*B*) Immediately after final watering.

Water uptake through the woody twigs of 15-year-old *Picea abies* (L.) Karst has been observed by Katz *et al.* (19). Dyes were shown to have migrated through the bark and bark parenchyma. If water uptake occurs through tree stems and twigs, a similar path for water uptake by woody roots seems probable. Additionally, in roots exhibiting advanced stages of secondary growth, the endodermis is no longer present to act as an ion or water barrier. The cambial layer may act to serve in that function; however, in *P. abies* dyes were seen to penetrate the cambium and to enter the woody tissue interior to the cambium.

In the present work, the presence of a water-depletion region surrounding the woody taproot that was not restricted to root junctions or wounds supports the hypothesis that suberized, woody roots play an important role in water absorption. The images presented here were scaled in image brightness to emphasize visualization of the water depletion region, diminishing the structural detail within the root tissue. In Fig. 5, however, there are clearly concentric rings visible within the taproot, suggesting differences in either water content or water binding within specific root interior regions.

These experiments have demonstrated a noninvasive application of MRI to image water-depletion patterns in sand surrounding plant roots. A water-depletion region was seen to form around woody taproots of loblolly pine, providing evidence that roots that have undergone secondary growth are potential regions of water inflow into a loblolly pine seedling.

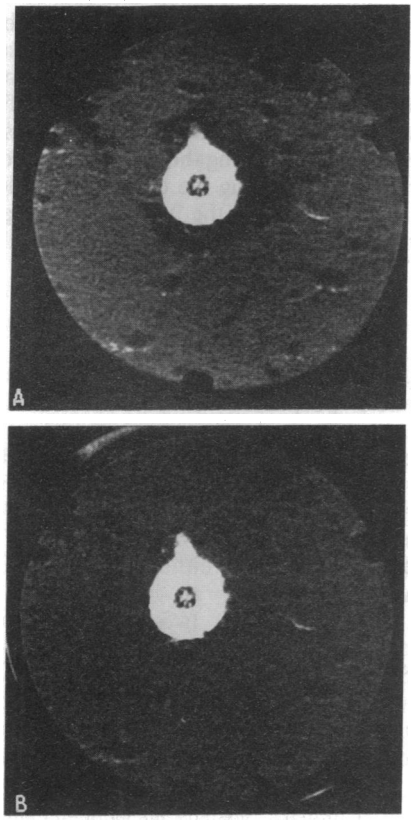

FIG. 7. Sequential images of loblolly pine taproot and excised lateral root. (*A*) At 24 hr after initial watering. (*B*) Immediately after final watering.

We gratefully acknowledge the technical contributions of Mr. Gary Cofer and we thank Drs. J. R. MacFall and J. Veres for their insightful suggestions and discussions during the progress of this work. We thank Drs. R. Oren, D. Richter, B. Strain, and B. Osmond for critical review of the manuscript. We also thank Mr. Steve Suddarth, Ms. Sharon Ziv, and Ms. Linda Werrell for technical assistance.

1. Kramer, P. J. & Bullock, H. C. (1966) *Am. J. Bot.* **53,** 200–204.
2. Chung, H. H. & Kramer, P. J. (1975) *Can. J. For. Res.* **5,** 229–235.
3. Haussling, M., Jorns, C. A., Lehmbecker, G., Hecht-Bucholz, C. & Marchner, H.(1988) *J. Plant Physiol.* **133,** 486–491.
4. McCully, M. E. & Canny, M. J. (1988) *Plant Soil* **111,** 159–170.
5. Passioura, J. B. (1988) *Annu. Rev. Plant Physiol. Plant Mol. Biol.* **39,** 245–265.
6. Bottomley, P. A., Rogers, H. H. & Foster, T. H. (1986) *Proc. Natl. Acad. Sci. USA* **83,** 87–89.
7. Rogers, H. H. & Bottomley, P. A. (1987) *Agron. J.* **79,** 957–965.
8. Gadian, D. G. (1982) *Nuclear Magnetic Resonance and Its Applications to Living Systems* (Clarendon, Oxford).
9. Brown, J. M., Johnson, G. A. & Kramer, P. J. (1986) *Plant Physiol.* **82,** 1158–1160.
10. Connelly, A., Loughman, J. A. B., Loughman, B. C., Quiquampoix, H. & Ratcliffe, R. G. (1987) *J. Exp. Bot.* **38,** 1713–1723.
11. Johnson, G. A., Brown, J. & Kramer, P. J. (1987) *Proc. Natl. Acad. Sci. USA* **84,** 2752–2755.
12. Eccles, C. D., Callahan, P. T. & Jenner, C. F. (1988) *Biophys. J.* **53,** 77–81.
13. MacFall, J. R., Wehrli, F. W., Breger, R. K. & Johnson, G. A. (1987) *Magn. Reson. Imaging.* **5,** 209–220.
14. Fullerton, G. C., Potter, J. L. & Dornbluth, N. C. (1982) *Magn. Reson. Imaging* **1,** 209–228.
15. Herfkens, R., Davis, P., Crooks, L., Kaufman, L., Price, D., Miller, T., Marqulis, A., Watts, J., Joenninger, J., Arakawa, M. & McRee, R. (1981) *Radiology* **141,** 211–218.
16. Wehrli, F. W., MacFall, J. R. & Newton, T. H. (1983) in *Advanced Imaging Techniques*, eds. Newton, T. H. & Potts, D. G. (Clavadel, San Anselmo, CA), Vol. 2, pp. 81–117.
17. Reed, J. F. (1939) *Root and Shoot Growth of Shortleaf and Loblolly Pines in Relation to Certain Environmental Conditions* (School of Forestry, Duke Univ., Durham, NC) Bull. 4.
18. Wahlenberg, W. G. (1960) *Loblolly Pine* (School of Forestry, Duke Univ., Durham, NC).
19. Katz, C., Øren, R., Schulze, E. D. & Milburn, J. A. (1989) *Trees* **3,** 33–37.

Downloaded at Palestinian Territory, occupied on November 28, 2021